



Published in final edited form as:

Nat Med. 2013 June ; 19(6): 695–703. doi:10.1038/nm.3155.

Chemotherapy-induced bone marrow nerve injury impairs hematopoietic regeneration

Daniel Lucas¹, Christoph Scheiermann^{1,*}, Andrew Chow^{1,2}, Yuya Kunisaki¹, Ingmar Bruns^{1,3}, Colleen Barrick⁴, Lino Tessarollo⁴, and Paul S. Frenette^{1,2}

¹Ruth L. and David S. Gottesman Institute for Stem Cell and Regenerative Medicine Research, Albert Einstein College of Medicine, New York, NY 10461, USA

²Mount Sinai School of Medicine, New York, NY 10029, USA

³Department of Hematology, Oncology and Clinical Immunology, Heinrich Heine University, Moorenstr. 5, 40225 Dusseldorf, Germany

⁴Mouse Cancer Genetics Program, Center for Cancer Research, NCI-Frederick, Frederick, MD 21702, USA

Abstract

Anti-cancer chemotherapy drugs challenge hematopoietic tissues to regenerate, but commonly produce long-term sequelae. Deficits in hematopoietic stem or stromal cell function have been described, but the mechanisms mediating chemotherapy-induced hematopoietic dysfunction remain unclear. Administration of multiple cycles of cisplatin chemotherapy causes significant sensory neuropathy. Here, we demonstrate that chemotherapy-induced nerve injury in the bone marrow is a critical lesion impairing hematopoietic regeneration. We show using various pharmacological and genetic models that the selective loss of adrenergic innervation in the BM alters its regeneration following genotoxic insult. Sympathetic nerves in the marrow promote the survival of stem cell niche constituents that initiate recovery. Neuroprotection by deletion of *Trp53* in sympathetic neurons or neuro-regeneration using 4-methylcatechol or glial-derived neurotrophic factor (GDNF) administration can restore hematopoietic recovery. Thus, these results shed light on the potential benefit of adrenergic nerve protection to shield hematopoietic niches from injury.

The hematopoietic system continuously renews itself; billions of blood cells are produced every day in the bone marrow (BM) by the regulated proliferation and differentiation of

Users may view, print, copy, download and text and data- mine the content in such documents, for the purposes of academic research, subject always to the full Conditions of use: http://www.nature.com/authors/editorial_policies/license.html#terms

*Current address: Walter Brendel Centre of Experimental Medicine, Ludwig-Maximilians-Universität München, Marchioninistrasse 15, 81377 Munich, Germany

AUTHOR CONTRIBUTIONS

D. Lucas designed and performed experiments and wrote the paper. C. Scheiermann, A. Chow, I. Bruns. and Y. Kunisaki performed experiments and analyzed data. P.S.F. designed experiments and wrote the paper. C. Barrick and L. Tessarollo generated and provided *Tal-Cre:Trka^{neo/neo}* mice.

COMPETING FINANCIAL INTERESTS

The authors declare no competing financial interests. Correspondence and requests for materials should be addressed to P.S.F. (paul.frenette@einstein.yu.edu)

hematopoietic stem cells (HSC). In patients with cancer, chemotherapy frequently causes acute BM injury that leads to aplasia followed by extensive remodeling of the stromal compartment^{1–4}. In addition to the acute cytotoxicity, patients that have received prior chemotherapy often exhibit irreversible chronic BM damage producing impaired hematopoietic reserve and function, reduced granulocyte colony-stimulating factor (G-CSF)-induced mobilization of HSCs and delayed engraftment after transplantation^{4–8}. Functional defects in HSC and/or stromal cell activities have been reported following conventional chemotherapy^{3–5,7,9–11}, but the underlying mechanisms remain unresolved.

We have previously shown that the sympathetic nervous system (SNS) directs HSC trafficking by acting on nestin⁺ niche cells^{12,13}. Since several chemotherapeutic drugs (e.g. vinca alkaloids, taxanes, platinum-based) commonly induce severe peripheral neuropathies¹⁴, we hypothesized that chemotherapy-induced neuropathy in the bone marrow is a critical lesion preventing hematopoietic regeneration.

RESULTS

Neurotoxic chemotherapy impairs BM regeneration

We treated mice with seven cycles of cisplatin (Fig. 1a) to induce a sensory neuropathy similar to that observed clinically¹⁵. Four or eight weeks after the last injection bone marrow nucleated cells (BMNC), hematopoietic progenitors (CFU-C) and Lin⁻Sca1⁺c-kit⁺ cell counts (Supplementary Fig. 1a–f) had completely recovered. Cisplatin-induced neuropathy has been reported to largely affect sensory nerves¹⁵. In agreement, cisplatin-treated mice exhibited sensory neuropathy at this time (Fig. 1b). Following transplantation with fresh healthy BMNC, survival in the cisplatin-treated group was significantly impaired (by 33%, $P < 0.05$; Fig. 1c) due to reduced hematopoietic activity as shown by BM aplasia (Fig. 1d) and severe pancytopenia in moribund mice (Supplementary Table 1). Four weeks after transplantation, the BM of surviving cisplatin-treated mice was still severely aplastic, and showed dramatic reductions in progenitors and HSC-enriched Lin⁻Sca1⁺c-kit⁺Flt3⁻ cells (LSKF; Supplementary Fig. 2a–c). These results suggest that prior cisplatin treatment alters the host BM microenvironment, impairing hematopoietic recovery.

To further investigate the specificity of neurotoxic chemotherapy drugs, we compared cisplatin treatment with carboplatin, a non-neurotoxic drug of the same family, and vincristine, another classical neurotoxic chemotherapeutic agent. We assessed whether cisplatin and vincristine caused sympathetic neuropathy in the BM by staining for BM SNS fibers with an antibody against the catecholaminergic enzyme tyrosine hydroxylase (Th). Both drugs reduced the density of Th⁺ fibers by 80% compared with vehicle control (Fig. 1e–f). Furthermore, while the recovery of LSKF cells (Fig. 1g) and competitive HSC reconstitution capacity (Supplementary Table 2) were compromised after transplantation in cisplatin- and vincristine-treated mice, carboplatin-treated animals exhibited a recovery similar to that of controls (Fig. 1g), suggesting that sympathetic neurotoxicity was associated with poor hematopoietic recovery after genotoxic insult.

Sympathetic nerves are required for BM recovery

To evaluate more specifically whether sympathetic innervation was required for hematopoietic regeneration, we denervated the SNS by treatment with 6-hydroxydopamine (6OHDA). Consistent with previous studies^{12,16}, and in contrast to a recent report¹⁷, sympathectomy by itself did not alter BMNC, CFU-C or hematopoietic stem cell and progenitor content or cell cycle (Supplementary Fig. 3a–e). However, transplantation of wild-type BMNC into lethally irradiated 6OHDA- or saline-treated mice (Fig. 2a) led to a significant increase in mortality in the 6OHDA group (Fig. 2b) and delayed hematopoietic recovery 4 weeks post-transplantation (Fig. 2b and Supplementary Fig. 4a,b).

Transplantation of HSCs is a complex process that requires homing to the BM and migration to the appropriate niche for survival and proliferation¹⁸. Neither 6OHDA, nor cisplatin therapy affected progenitor homing to BM (Supplementary Fig. 5a–e). In addition, reduced BM recovery was also observed after challenging sympathectomized mice with sublethal irradiation (Supplementary Fig. 5f–i), further suggesting that reduced BM recovery was independent of homing. To confirm this issue, we also tested the response to 5-fluorouracil (5FU), which ablates proliferating cells while inducing quiescent HSCs to repopulate the BM *in situ*. 6OHDA-sympathectomized mice demonstrated dramatic reductions in survival upon 5FU challenge (Fig. 2c), due to hematopoietic failure (Fig. 2d; Supplementary Fig. 6a–f; Supplementary Table 3). Importantly, neither lethal irradiation nor 5FU treatment caused any detectable loss of Th⁺ nerve fibers (Supplementary Fig. 7a–d). These results suggest that SNS signals are required for HSC expansion and survival during BM recovery.

To confirm the role of the SNS in regeneration, we intercrossed *Th-Cre* mice¹⁹ (which express the CRE recombinase in catecholaminergic neurons) with *iDTR* mice²⁰ (in which CRE-mediated recombination induces expression of the diphtheria toxin receptor). Diphtheria toxin injection in *Th-Cre:iDTR* mice triggered apoptosis of peripheral sympathetic neurons (Fig. 2e). SNS injury was still evident in the BM of *Th-Cre:iDTR* mice 12 days after 5FU administration (Fig. 2f) and resulted in reduced hematopoietic regeneration (Fig. 2g and Supplementary Fig. 6g), further suggesting that an intact SNS was required for BM recovery. We next assessed which adrenergic receptors mediated bone marrow regeneration. Circadian physiological HSC release is largely controlled by the β 3 adrenergic receptors (β 3-AR) expressed by niche cells¹², whereas the β 2 adrenergic receptor (β 2-AR) is broadly expressed in non-hematopoietic and hematopoietic fractions, including human CD34⁺ cells where it regulates progenitor migration²¹. We found overlapping functions for β 2 and β 3 adrenergic receptors in BM recovery after 5FU, since a deficit similar to 6OHDA-sympathectomized mice was observed only when the function of both β -adrenergic receptors was inactivated (Fig. 2h and Supplementary Fig. 8).

Reduced BM recovery after cisplatin chemotherapy is due to SNS injury

Since deletion of the tumor suppressor *Trp53* in sympathetic neurons was reported to promote neuronal survival after genotoxic insult²², we hypothesized that Trp53-deficient SNS nerves would be protected from chemotherapy-induced injury and that this would be associated with improved hematopoietic recovery. To this end, we intercrossed *Th-Cre* mice with *Trp53^{fllox/fllox}* animals²³. As expected, peripheral sympathetic neurons from cisplatin-

treated *Th-CreTrp53*^{-/-} mice did not express Trp53 after cisplatin treatment (Supplementary Fig. 9). This led to reduced apoptosis after cisplatin (Fig. 3a) and increased numbers of BM SNS fibers in *Th-Cre;Trp53*^{-/-} mice at the end of the cisplatin protocol (Fig. 3b,c).

We then subjected *Th-Cre;Trp53*^{-/-} mice and control littermates to cisplatin treatment followed by transplantation (as in Fig. 1a). Remarkably, we found improved survival and hematopoietic recovery (Fig. 3d,e) in cisplatin-treated *Th-Cre;Trp53*^{-/-} mice when compared to cisplatin-treated control littermates. Thus, these results strongly support the notion that chemotherapy-induced SNS injury impairs hematopoietic regeneration after transplantation.

β-adrenergic signals promote niche cell survival

We further investigated the mechanisms through which the SNS promoted BM regeneration. Since LSKF cells failed to expand in SNS-injured mice (Fig. 1g and Fig. 2c,g,h) and the SNS targets Nestin-expressing niche cells to regulate HSC trafficking¹³, we hypothesized that the SNS is required for niche recovery after genotoxic insult. We thus treated *Nes-Gfp* mice with 6OHDA and assessed regeneration following 5FU challenge. Twelve days after 5FU challenge, the BM of 6OHDA-mice contained fewer Nestin-GFP⁺ cells and CD31⁺ endothelial cells (EC), which contribute to the HSC niches^{13,24,25}, compared to 5FU-treated controls (Fig. 4a,b). No significant change was noted in bone osteoblasts or BM macrophages (Supplementary Fig. 10a–g). We then treated *Nes-Gfp* mice with SR59230A (β₃-AR antagonist) and ICI118551 (β₂-AR antagonist) for three consecutive days followed by 5FU. Twelve days later, we found reduced numbers of Nestin-GFP⁺ cells and CD31⁺ endothelial cells (EC) after pharmacological β-adrenergic blockade (Fig. 4c,d). Similar results were obtained in cisplatin-treated *Nes-Gfp* mice 4 weeks after transplantation (Fig. 4e,f). Since β-adrenergic antagonists were administered prior 5FU injection, our results suggest that the SNS acts acutely to protect niche constituents from genotoxic insult. Indeed, the number of Nestin-GFP⁺ cells and CD31⁺ EC in 6OHDA- or β₂/β₃-antagonist-treated mice was reduced as early as 24h after 5FU injection (Fig. 4g,h). Taken together, these data indicate that the SNS promotes hematopoietic function by protecting Nestin-GFP⁺ cells and EC from genotoxic insult.

SNS injury itself did not alter BMNC, CFU-C or LSKF content but increased the number of Nestin-GFP⁺ cells (Supplementary Fig. 10h,j,k). Further, β₂/β₃-antagonist-treatment increased proliferation of Nestin-GFP⁺ and endothelial cells (Supplementary Fig. 10i). These results suggest that the SNS negatively regulates the size of the HSC niche. To confirm that SNS injury does not impair steady-state niche function, we transplanted 6OHDA or cisplatin-treated CD45.2 mice with 10⁷ BMNC from CD45.1⁺ mice without irradiation. Unexpectedly, we observed an enhanced multilineage engraftment in 6OHDA or cisplatin-treated mice without other conditioning (Supplementary Fig. 11a,b). The engraftment was sustained for 16 weeks in cisplatin- but not 6OHDA-treated group, likely due to the rapidly reversible (~2 weeks) injury of 6OHDA. The fact that the enhanced engraftment correlates with the increase in Nestin-GFP⁺ cell numbers (Supplementary Fig. 10h,k) suggests that the expanded niches were functional and capable to support transplanted HSC.

Chemotherapy-induced SNS injury impairs HSC mobilization

After acute administration of chemotherapy, hematopoietic recovery can be accompanied by a marked mobilization of HSC/progenitors in the bloodstream, suggesting that the mobilization process may be associated with marrow regeneration²⁶. Since the SNS regulates HSC egress^{12,16}, we tested the possibility that poor mobilization from prior chemotherapy treatment in cancer patients⁵ could be caused by BM neuropathy. We treated mice weekly with saline or cisplatin for 7 weeks, and induced HSC/progenitor mobilization with G-CSF after the 4-week recovery period (Fig. 5a). Cisplatin-treated mice exhibited a ~50% reduction in the number of mobilized CFU-C, LSKF and long-term culture-initiating cells (LTC-IC) in the blood (Fig. 5b and Supplementary Table 4). Further, competitive repopulation experiments revealed reduced HSC content in G-CSF-mobilized blood of cisplatin-treated mice (Fig. 5c). No significant changes in progenitors or LSKF cells (Fig. 5d) were detected in the BM of these animals, indicating that the reduced mobilization was not due to lower numbers of HSC/progenitors from chemotherapy treatment.

To exclude the possibility of an HSC-autonomous defect, cisplatin and saline-treated mice were lethally irradiated and transplanted with fresh wild-type BMNC and allowed to recover for 16 weeks (Fig. 5e). At this time point, BM recovery was complete, and HSC content (as determined by competitive reconstitution with limiting dilution) was similar in cisplatin- or saline-treated mice (Supplementary Fig. 12a,b and Supplementary Table 5). However, there was still a ~50% reduction in mobilization efficiency after G-CSF in cisplatin-treated mice compared to saline-treated control animals (Fig. 5f,g), indicating that cisplatin treatment produces bone marrow neuropathy which markedly compromises G-CSF-induced mobilization.

Neuroprotection rescues BM function after chemotherapy

Based on these results, we predicted that interventions that protect neural function might also restore hematopoietic regeneration. We engineered a chimeric molecule by fusion of the C-terminal end of the murine *glial cell-derived neurotrophic factor* gene (*Gdnf*), which was reported to rescue preganglionic sympathetic neurons after adrenalectomy²⁷, with the human IgG1 Fc region. Purified GDNF-Fc was able to induce neural differentiation of PC12ES cells, thus demonstrating its activity *in vitro* (Supplementary Fig. 13a). GDNF-Fc administration to cisplatin-treated mice reduced sensory neuropathy (Supplementary Fig. 13b,c) and led to increased survival after transplantation, accelerated BM recovery, and increased BM Th⁺ fibers when compared to mice treated with cisplatin alone (Supplementary Fig. 13b–h). Similar results were observed in the 5FU model where GDNF-Fc administration promoted survival and accelerated BM recovery in 6OHDA-treated mice (Supplementary Fig. 14a–c).

Next, we administered 4-methylcatechol (4-MC), a drug reported to induce endogenous nerve growth factor (NGF) production and to protect SNS fibers^{28,29}, during the 7 cycles of cisplatin chemotherapy. This treatment reduced sensory neuropathy (Supplementary Fig. 15a) and restored normal fiber density of BM Th⁺ nerves in cisplatin and 4-MC compared to cisplatin & saline control group (Fig. 6a). Moreover, 4-MC treatment enhanced survival (Fig. 6b; $P < 0.05$ Logrank test) and accelerated bone marrow regeneration after

transplantation (Fig. 6c and Supplementary Fig. 15b,c) and significantly increased BM HSC frequency (Supplementary Table 6). 4-MC treatment also restored normal numbers of Nestin-GFP⁺ and endothelial cells in cisplatin-treated mice (Fig. 6c). These results indicate that neuroprotection from cisplatin-induced SNS injury by 4-MC accelerates BM regeneration. To evaluate further whether the effect of 4-MC was specifically due to the recovery of SNS fibers, we administered 4-MC in mice in which the SNS was lesioned with 6OHDA, and analyzed BM regeneration after 5FU injection. We found that 4-MC administration also protected Th⁺ fibers (Supplementary Fig. 16a), promoted hematopoietic recovery (Fig. 6d,e and Supplementary Fig. 16b,c), and completely protected mice from death due to BM aplasia (Fig. 6e). 4-MC also increased HSC recovery as measured by LTC-IC assay (Supplementary Table 7), and restored the numbers of Nestin-GFP⁺ cells and CD31⁺ endothelial cells 12 days after 5FU (Fig. 6f), without affecting BM macrophage or bone osteoblast numbers (Supplementary Fig. 17a–e). Taken together, these results clearly show that neuroprotection can enhance BM recovery after SNS injury, probably by maintaining the ability of the SNS to promote survival of niche cells after genotoxic insult.

NGF signals via two receptors, the p75 low affinity receptor and TrkA. TrkA appears to be the dominant receptor because the phenotype of *TrkA*^{-/-} mice resembles that of *Ngf*^{-/-} animals^{30,31}. However, TrkA is not exclusively expressed in neurons but also in non-neural stromal cells³². To investigate whether the effect of 4-MC on BM recovery was specifically due to protection of neurons, we analyzed *Tal-Cre:TrkA^{Neo/Neo}* mice, in which TrkA is expressed exclusively in neurons but not in other tissues³³. Sympathectomized *Tal-Cre:TrkA^{Neo/Neo}* mice treated with 4-MC exhibited a recovery comparable to sympathectomized control mice treated with 4-MC (Fig. 6g and Supplementary Fig. 18), suggesting that the action of 4-MC was mediated via TrkA signaling in neurons.

To evaluate further the effect of neuroprotection in a clinically relevant setting, we analyzed whether 4-MC or GDNF-Fc treatment could restore G-CSF-induced mobilization in cisplatin-treated mice. As observed earlier (Fig. 5b), the numbers of G-CSF-mobilized progenitors and LSKF cells in blood were markedly reduced in the group treated with cisplatin (Fig. 6h). In contrast, G-CSF-induced mobilization was restored after neuroprotection with 4-MC (Fig. 6h) or GDNF-Fc (Supplementary Fig. 19). Thus, 4-MC maintains hematopoietic function by specifically protecting SNS fibers in the BM, offering a novel avenue for clinical intervention.

DISCUSSION

Here, we show that neurotoxicity from anti-cancer chemotherapy impairs bone marrow regeneration after transplantation. Our results suggest that SNS signaling exerts critical functions immediately after genotoxic insult (e.g. irradiation or 5FU) to promote survival of niche constituents, thereby promoting efficient hematopoietic recovery. Our data support the notion that neurotoxic chemotherapy agents can damage autonomic nerves in the bone marrow and compromise HSC mobilization and hematopoietic regeneration. These studies provide the proof-of-principle that neuroprotection may preserve hematopoietic and mobilization reserves after neurotoxic chemotherapy.

Recent studies have identified the vasculature, including endothelial cells³⁴, Cxcl12-abundant reticular (CAR) cells³⁵, Nestin⁺ mesenchymal stem cells¹³, and leptin receptor expressing cells²⁵, as a potential niche for HSC in the bone marrow³⁶. Interestingly, our results indicate that Nestin⁺ and endothelial cells follow similar recovery kinetics after BM injury. The fact that autonomic nerves and perivascular stromal cells are linked by gap junctions³⁷ could contribute to the synchronized response of the vascular niche. The gap junction protein Connexin43 is indeed required for efficient BM regeneration³⁸. Further, endothelial cells and pericyte are known to have intricate interactions involving paracrine or juxtacrine signaling³⁹. For example, pericytes promote endothelial cell survival by inducing an autocrine VEGF loop in the endothelial cell⁴⁰ and VEGF signaling is critical for BM regeneration¹. Similarly, endothelial cell-derived PDGF-B is required for pericyte recruitment to blood vessels during angiogenesis³⁹. Further studies will be needed to evaluate in greater detail the exact stromal cell(s) targeted by the SNS.

While our results clearly indicate that neural signals are critical for HSC niche recovery, they also point to chemotherapy injury (in the case of cisplatin) to stromal cells outside of the HSC niche since neuroprotection allowed full HSC recovery but differential benefits in the recovery of clonogenic progenitors or total BM cellularity compared to 6OHDA-lesioned animals. This possibility is also suggested by differences in recovery of HSC and total BM cells between vincristine and cisplatin. The present study, however, strongly support the notion that cisplatin-induced neuropathy alters niche function after stress, and that under homeostasis, SNS signals in the bone marrow can negatively regulate niche size.

Although much of the attention for chemotherapy-induced neuropathy has been devoted to the most clinically visible sensory neural dysfunctions⁴¹, our results highlight an insidious form of autonomic neuropathy of the bone marrow which may present a risk for patients requiring further intensive therapy (e.g. bone marrow transplantation). Thus, neuroprotective agents coupled with conventional chemotherapy may prevent long-term bone marrow injury and provide additional therapeutic options to previously treated cancer patients.

Online Methods

Mice

Six to seven week old female C57BL/6J mice were purchased from the National Cancer Institute (NCI, Frederick Cancer Research Center, Frederick, Maryland). *Adrb2^{tm1Bkk/J}* mice⁴² were a gift from Dr. Gerard Karsenty. *B6.SJL^{Ptprca Pep3b/BoyJ} (SJL)*, *B6.Cg-Tg(Thcre)1Tmd/J (Th-Cre)*¹⁹, *B6.129P2-Trp53^{tm1Brn/J} (Trp53^{flox/flox})* mice²³ and *C57BL/6-Gt(ROSA)26-Sor^{<tm1(HBEGF)Awai>/J} (iDTR)*²⁰ were purchased from the Jackson laboratory. *Ta1-Cre:Trka^{neo/neo}* mice were described previously³³. *Nestin-gfp* mice were described previously⁴³. All mice were housed at the Center for Comparative Medicine and Surgery at Mount Sinai School of Medicine (MSSM) or the institute for Animal Studies at Albert Einstein College of Medicine (AECOM). The Animal Care and Use Committee of MSSM and the Institutional Animal Care and Use Committee of AECOM approved experimental procedures performed on mice. Due to the circadian regulation of HSC trafficking¹³ and mobilization⁴⁴ all experiments were performed between 5 and 8 hours after the onset of light (Zeitgeber time 5–8).

6-hydroxydopamine (6OHDA) treatment

To induce acute peripheral sympathectomy, mice received two i.p. injections of 6OHDA (Sigma; 100 mg kg⁻¹ on day 0; 250 mg kg⁻¹ on day 2). Three days after the last injection of 6OHDA mice were euthanized for analysis, subjected to transplantation, or injected with 5-fluorouracil.

Chemotherapy treatment

To assess the role of chemotherapy in bone marrow transplantation, mice were injected i.p. with cisplatin (10 mg kg⁻¹; once per week; Teva), carboplatin (30 mg kg⁻¹; once per week; Sigma) or vincristine (0.125 mg kg⁻¹; twice per week; Sigma) for 6 (vincristine) or 7 (cisplatin and carboplatin) weeks as described^{15,45}. Four weeks after the last injection of chemotherapy (to allow full BM recovery), mice were euthanized for analysis, transplanted as above or mobilized with granulocyte colony-stimulating factor (G-CSF).

Bone marrow transplantation in non-conditioned mice

To assess niche function after 6OHDA-sympathectomy mice were treated with saline or 6OHDA and 3 days later injected with 10⁷ BMNC from CD45.1⁺ (SJL) mice. Four weeks later the percentage of CD45.1⁺ positive cells present in the blood was measured by flow cytometry. To determine the effect of cisplatin in niche function in steady-state mice were treated with saline or cisplatin and 4 weeks later injected with 10⁷ BMNC from CD45.1⁺ (SJL) mice and analyzed 4 weeks later as above.

Bone marrow transplantation after irradiation conditioning and HSC quantification

Mice were irradiated (1,200 cGy, two split doses, 3 h apart) in a Cesium Mark 1 irradiator (JL Sheppard & associates), 3 h after the last dose, the indicated number of BMNCs was injected retroorbitally under isoflurane (Phoenix pharmaceuticals) anesthesia. Mice were allowed to recover and analyzed at the indicated time points. For competitive repopulation assays from BM cells, 10⁵ BMNC from the donor BM were injected together with 10⁵ CD45.1⁺ competitor BMNC into lethally irradiated recipients. Sixteen weeks later the percentage of donor-derived cells was determined as described⁴⁶.

For competitive repopulation assays we injected 10 µl of G-CSF mobilized blood (CD45.2⁺) along with 2.5 × 10⁵ CD45.1⁺ competitor BMNC into lethally irradiated SJL recipients (CD45.1⁺). Sixteen weeks later, we quantified the percentage of CD45.2⁺ cells in the blood of the recipient mice. In one experiment saline- or cisplatin-treated mice were first transplanted with 10⁶ fresh BMNC from congenic SJL mice (CD45.1⁺). Sixteen weeks later, the transplanted mice were mobilized with G-CSF and the number of HSC quantified by competitive repopulation: we transplanted 90 µl from the mobilized blood (CD45.1⁺ as is derived from the SJL cells in the first transplant) along with 1.5 × 10⁵ CD45.2⁺ competitor BMNC into lethally irradiated C57BL/6 recipients (CD45.2⁺). Sixteen weeks later we measured the percentage of CD45.1⁺ cells in the blood of the transplanted mice.

Repopulating units were calculated as described⁴⁷. To determine competitive repopulating units (CRU) serial dilutions of donor BMNC were injected together with 2 × 10⁵ CD45.1⁺ competitor BMNC from SJL mice into lethally irradiated SJL recipients. Sixteen weeks after

transplantation, the percentage of donor-derived cells was determined as described⁴⁶. Mice showing more than 1% trilineage reconstitution were considered positive. To determine long-term cell-initiating culture (LTC-IC) numbers, serial dilutions of blood or BMNC were plated on single well stromal cultures; 4 weeks later each individual well was assayed for the presence of CFU-C as described⁴⁶.

G-CSF-induced mobilization

Mice received G-CSF (250 mg kg⁻¹ day⁻¹) s.c. every 12 h for 5 days. Due to circadian oscillations on HSC mobilization⁴⁴, the last dose of G-CSF was administered 1 h before blood collection at Zeitgeber time 5.

5-fluorouracil (5FU) treatment

To induce bone marrow ablation and force quiescent HSC to proliferate, we injected 5FU (250 mg kg⁻¹; Sigma) i.v. under isoflurane (Phoenix pharmaceuticals) anesthesia. Mice were allowed to recover and analyzed at the indicated time points.

Diphtheria toxin (DT) treatment

To induce acute peripheral sympathectomy, *Th-Cre:iDTR* or Control (wild-type, *Th-Cre* or *iDTR*) mice received two i.p. injections of DT (0.1 ng kg⁻¹) on day 0 and day 2. Three days after the last injection of DT mice were injected with 5FU.

Sublethal irradiation

Mice were irradiated with a single dose of 800 rads in a Cesium Mark 1 irradiator (JL Sheppard & associates).

Inhibition of β adrenergic receptors *in vivo*

To investigate the role of β 2 or β 3 adrenergic receptors in bone marrow regeneration, we inactivated β 2- β 3 adrenergic signaling in wild-type or *Adrb2*^{tm1Bkk/J} mice by injecting the β 3 specific antagonist SR59230A (5 mg kg⁻¹, i.p.; Sigma) or the β 2 specific antagonist ICI118,551 hydrochloride (1 mg kg⁻¹, i.p.; Sigma), daily for 3 days. For simultaneous β 2- β 3 pharmacological blockade SR59230A and ICI 118,551 were injected 3 h apart to minimize drug interactions.

Generation of GDNF-Fc

The murine cDNA for glial cell-line derived neurotrophic factor (*Gdnf*) was obtained from Open Biosystems. cDNA was amplified and restriction sites were added for cloning with the following primers Forward: ACG CTA GCA ATG GGA TTC GGG CCA CTT; Reverse: CGA GAT CTG CGA TAC ATC CAC ACC GTT TAG. The PCR product was purified and cloned into the PCL5.1neg plasmid to generate PCL5.1neg-GDNF. This plasmid was purified and transfected into 293T cells. Two days after transfection, the supernatant was collected and GDNF-Fc purified in a Protein G-sepharose column (Pierce). To assess functional activity of GDFN-Fc recombinant protein we cultured PC12ES cells in DMEM supplemented with 5% FBS, 10% horse serum, sodium-pyruvate (Gibco), L-Glutamine (Gibco) and penicillin/streptomycin (Gibco) for 3 days and then replaced the media with

DMEM supplemented with 1% horse serum, sodium-pyruvate (Gibco), L-Glutamine (Gibco), penicillin/streptomycin (Gibco) and varying amounts of GDNF-Fc to induce differentiation. Seven days later the percentage of PC12 ES with two or more dendrites was scored under an inverted microscope. For each concentration of GDNF-Fc 10 fields were analyzed.

Neuroprotection with 4-methylcatechol (4-MC) or GDNF-Fc

To induce neuroprotection from cisplatin, mice were injected i.p. with 4-MC ($10 \mu\text{g kg}^{-1}$; Sigma) daily for the 7 weeks of cisplatin treatment as described²⁹. We also induced neuroprotection in cisplatin-treated mice with daily s.c. injections of recombinant GDNF-Fc ($5 \mu\text{g}$ per mice) during 2 weeks immediately after the last injection of cisplatin. To induce neuroprotection from 6OHDA, mice were injected with 4-MC ($10 \mu\text{g kg}^{-1}$; i.p.) or GDNF-Fc ($5 \mu\text{g}$ per mice; s.c.) for 5 days starting the treatment the same day as the first injection of 6OHDA.

Blood, spleen, bone and bone marrow analyses

Blood was harvested by retro-orbital sampling of mice anesthetized with isofluorane and collected in polypropylene tubes containing ethylenediaminetetraacetic acid (EDTA). Blood parameters were determined with Advia 120 Hematology System (Siemens). CFU-C assays were performed as described in¹⁶. Bone marrow was harvested by flushing the bone with 1 mL of ice-cold PBS, red blood cells were lysed once for 5 min at 4 oC in NH_4Cl 0.15 M, cells were washed once in ice cold PBS and counted with a hemocytometer. For flow cytometry, red blood cells were lysed thrice for 5 min at 4 oC in NH_4Cl 0.15 M, cells were washed once in ice cold PBS and counted in a hemocytometer. For LSK and LSKF detection, 10^6 cells were stained with the Mouse Lineage Panel (eBioscience Cat No: 88-7774-75; 1:50 dilution) together with FITC-conjugated anti-Sca-1 (eBioscience Cat No: 11-5981-85), PE-Cy7-conjugated anti-c-kit (eBioscience Cat No: 25-1171-82) and PE-conjugated anti-flt3 (eBioscience Cat No: 25-1171-82). Cells were further stained with streptavidin-Alexa647 (Jackson ImmunoResearch Cat No: 016-600-084). Macrophages were detected by staining with anti-CD115 (eBiosciences Cat No:12-1152-82), anti-Gr-1 (eBiosciences Cat no: 11-5931-85) and anti-F4/80 (Biolegend Cat No: 123122) as described⁴⁸. For endothelial cell and nestin⁺ cell quantification, $4-6 \times 10^6$ BM cells were resuspended in RPMI containing 10% Fetal Bovine Serum (FBS) and Collagenase type IV (0.2 mg ml^{-1} ; Sigma) and incubated at 37 oC for 30 min. Cells were then stained with anti-CD45 (eBioscience), anti-Ter119 (eBioscience) and anti-CD31 (eBioscience). For osteoblasts detection, the BM was flushed out of the bones and then chopped to small fragments and incubated in RPMI containing Collagenase type I (3 mg ml^{-1} ; Sigma) and incubated at 37 oC for 40 min. Cells were separated from the bone chips by filtering through a 35 mm mesh (BD Falcon) and stained with anti-CD45 (eBioscience Cat No: 47-0451-82), anti-Ter119 (eBioscience Cat No: 47-5921-82), anti-CD31 (Biolegend Cat No: 102516), anti-Sca1 (Biolegend Cat No:102516), and anti-CD51 (eBioscience Cat No: 12-0512-83). Stained cells were analyzed in a BD LSRII system (BD Biosciences). Unless otherwise specified all antibodies were used at a 1:100 dilution.

Annexin V staining and Cell cycle analyses

For HSC cell cycle experiments, 48h and 24h before analysis, mice received i.p. injections of BrdU (100 μ g; BD Biosciences). Mice were euthanized and BMNC purified and stained as indicated above. Cell cycle was determined by staining for BrdU-labeled cells with the APC BrdU Flow Kit (BD Biosciences) following manufacturer's instructions. Cells were then analyzed in a BD LSRII system (BD Biosciences). For apoptosis analyses, BMNC were purified and stained as indicated above and then further stained with the Annexin V-PE Apoptosis detection kit (BD Biosciences) or the Annexin V-APC Apoptosis detection kit (eBioscience) following manufacturer's instructions. For cell cycle analyses of niche components the bone marrow was digested with collagenase followed by antibody stain as above. Cells were then fixed in 2% paraformaldehyde in PBS, washed, permeabilized with 0.1% TritonX100, and stained with anti-Ki67-APC (eBiosciences Cat No: 51-5698-82) or an isotype control APC conjugate and Hoechst 33342 (Molecular Probes) at 20 mg mL⁻¹ for 30 min. After washing, cells were analyzed on a LSR II Flow Cytometer (Becton Dickinson).

Quantification of sensory neuropathy by the heated pad assay

To evaluate the effect of the different treatments on the sensory response, we performed the hot-plate test as described¹⁵. We used a Isotemp Dryblock (Fisher Scientific) maintained at 50 oC. Mice were individually placed on top of the heated surface and the time to the first episode of nociception (jumping or paw licking) measured. The cut-off time was of 60 s. Between measurements, the heated surface was thoroughly cleaned with detergent and ethanol and the temperature was allowed to stabilize to 50 oC.

Immunofluorescence analyses

Bones or superior cervical ganglia (SCG) were collected and fixed for 1 h in 4% paraformaldehyde (PFA) in PBS (Electron Microscopy Sciences) at 4 oC. They were then post-fixed overnight in 1% PFA in PBS at 4 oC. Bones were decalcified in EDTA 0.5 M for up to 2 weeks. Bones were then cryoprotected for 48 h in 15–30% sucrose. Organs were then included in OCT (Tissue Tek), sectioned in a Cryostat (SCG: 5 μ m sections; Bones 8 μ m sections) using the CryoJane tape system (Leica) and mounted on CFSA 4X Slides (Leica). Th⁺ immunofluorescence staining was performed as previously described¹². For each mouse analyzed the number of nerve fibers in 6 fields was quantified and plotted as per mm². Phospho-p53 immunofluorescence staining was performed with Anti-Phospho-p53 (Ser15) (Cell Signaling Technologies Cat No: 9284S; 1:50 dilution) following manufacturer's instructions followed by signal amplification with the TSA Plus Cyanine3 System (Perkin Elmer). TUNEL assay was performed using the In Situ Cell Death Detection Kit, TMR red (Roche) following manufacturer's instructions. For whole-mount immunofluorescence, calvaria were harvested by cutting along the temporal lines of the skull and immediately fixed in methanol. Bone tissues were blocked/permeabilized in PBS containing 20% FCS and 0.5% Triton and stained with anti-CD31 (Biolegend Cat No: 102516; 1:50 dilution) or anti-VE-cadherin (Biolegend Cat No: 138006; 1:50 dilution) and anti-Th (Millipore Cat No: AB152; 1:50 dilution) followed by signal amplification with the TSA Plus Cyanine3 System (Perkin Elmer). Whole-mount tissues were imaged face down on an upright Olympus BX61WI microscope. The area between the frontal and parietal

bones was identified by moving along the coronal suture, and images were obtained from the same area for all mice, along the coronal vein on either side of the central vein. The numbers of individual nerve fibers running alongside blood vessels were quantified and plotted as per 100 μm vessel segment. All images were processed using Slidebook software (Intelligent Imaging Innovations).

Statistical analyses

All data are represented as mean \pm standard error of the mean. Unless otherwise indicated comparisons between two samples were done using the Student's *t* test. Log Rank analyses were used for Kaplan-Meier survival curves. Analyses were performed using GraphPad Prism software (GraphPad Software). LTC-IC and CRU frequencies were calculated using L-Calc software (Stem Cell Technologies) * $P < 0.05$; ** $P < 0.01$; *** $P < 0.001$; ns: non significant.

Supplementary Material

Refer to Web version on PubMed Central for supplementary material.

Acknowledgments

We thank C. Prophete, M. Huggins and N. Dholakia for technical assistance. We thank Dr. Keisuke Ito for helpful discussions. This work was supported by the US National Institutes of Health (R01 grants DK056638, HL069438). D. Lucas was a fellow of Fundaci3n Ram3n Areces. C. Scheiermann was supported by a fellowship from the German Academic Exchange Service (DAAD). A. Chow is funded by a fellowship from the US National Institutes of Health (NIH) NHLBI 5F30HL099028-02. I. Bruns was the recipient of an American Society of Hematology–European Hematology Association (ASH-EHA) research exchange award. Y. Kunisaki was supported by the Japan Society for the Promotion of Science (JSPS). C. Barrick and L. Tessarollo are supported by the NIH intramural research program, Center for Cancer Research, NCI.

References

1. Hooper AT, et al. Engraftment and reconstitution of hematopoiesis is dependent on VEGFR2-mediated regeneration of sinusoidal endothelial cells. *Cell Stem Cell*. 2009; 4:263–274. [PubMed: 19265665]
2. Banfi A, et al. High-dose chemotherapy shows a dose-dependent toxicity to bone marrow osteoprogenitors: a mechanism for post-bone marrow transplantation osteopenia. *Cancer*. 2001; 92:2419–2428. [PubMed: 11745299]
3. Dominici M, et al. Restoration and reversible expansion of the osteoblastic hematopoietic stem cell niche after marrow radioablation. *Blood*. 2009
4. Mauch P, et al. Hematopoietic stem cell compartment: acute and late effects of radiation therapy and chemotherapy. *Int J Radiat Oncol Biol Phys*. 1995; 31:1319–1339. [PubMed: 7713791]
5. Haas R, et al. Patient characteristics associated with successful mobilizing and autografting of peripheral blood progenitor cells in malignant lymphoma. *Blood*. 1994; 83:3787–3794. [PubMed: 7515721]
6. Tricot G, et al. Peripheral blood stem cell transplants for multiple myeloma: identification of favorable variables for rapid engraftment in 225 patients. *Blood*. 1995; 85:588–596. [PubMed: 7529066]
7. Robinson SN, Freedman AS, Neuberg DS, Nadler LM, Mauch PM. Loss of marrow reserve from dose-intensified chemotherapy results in impaired hematopoietic reconstitution after autologous transplantation: CD34(+), CD34(+)/38(–), and week-6 CAFC assays predict poor engraftment. *Exp Hematol*. 2000; 28:1325–1333. [PubMed: 11146154]

8. Perseghin P, et al. Management of poor peripheral blood stem cell mobilization: incidence, predictive factors, alternative strategies and outcome. A retrospective analysis on 2177 patients from three major Italian institutions. *Transfus Apher Sci.* 2009; 41:33–37. [PubMed: 19540167]
9. Noach EJ, et al. Chemotherapy prior to autologous bone marrow transplantation impairs long-term engraftment in mice. *Exp Hematol.* 2003; 31:528–534. [PubMed: 12829029]
10. Galotto M, et al. Stromal damage as consequence of high-dose chemo/radiotherapy in bone marrow transplant recipients. *Exp Hematol.* 1999; 27:1460–1466. [PubMed: 10480437]
11. Kemp K, et al. Chemotherapy-induced mesenchymal stem cell damage in patients with hematological malignancy. *Ann Hematol.* 2010; 89:701–713. [PubMed: 20119670]
12. Mendez-Ferrer S, Lucas D, Battista M, Frenette PS. Haematopoietic stem cell release is regulated by circadian oscillations. *Nature.* 2008; 452:442–447. [PubMed: 18256599]
13. Mendez-Ferrer S, et al. Mesenchymal and haematopoietic stem cells form a unique bone marrow niche. *Nature.* 2010; 466:829–834. [PubMed: 20703299]
14. Cavaletti G, Marmiroli P. Chemotherapy-induced peripheral neurotoxicity. *Nat Rev Neurol.* 2010; 6:657–666. [PubMed: 21060341]
15. Aloe L, Manni L, Properzi F, De Santis S, Fiore M. Evidence that nerve growth factor promotes the recovery of peripheral neuropathy induced in mice by cisplatin: behavioral, structural and biochemical analysis. *Auton Neurosci.* 2000; 86:84–93. [PubMed: 11269929]
16. Katayama Y, et al. Signals from the sympathetic nervous system regulate hematopoietic stem cell egress from bone marrow. *Cell.* 2006; 124:407–421. [PubMed: 16439213]
17. Yamazaki S, et al. Nonmyelinating Schwann cells maintain hematopoietic stem cell hibernation in the bone marrow niche. *Cell.* 2011; 147:1146–1158. [PubMed: 22118468]
18. Lapidot T, Dar A, Kollet O. How do stem cells find their way home? *Blood.* 2005; 106:1901–1910. [PubMed: 15890683]
19. Savitt JM, Jang SS, Mu W, Dawson VL, Dawson TM. Bcl-x is required for proper development of the mouse substantia nigra. *J Neurosci.* 2005; 25:6721–6728. [PubMed: 16033881]
20. Buch T, et al. A Cre-inducible diphtheria toxin receptor mediates cell lineage ablation after toxin administration. *Nat Methods.* 2005; 2:419–426. [PubMed: 15908920]
21. Spiegel A, et al. Catecholaminergic neurotransmitters regulate migration and repopulation of immature human CD34+ cells through Wnt signaling. *Nat Immunol.* 2007; 8:1123–1131. [PubMed: 17828268]
22. Trimmer PA, Smith TS, Jung AB, Bennett JP Jr. Dopamine neurons from transgenic mice with a knockout of the p53 gene resist MPTP neurotoxicity. *Neurodegeneration.* 1996; 5:233–239. [PubMed: 8910901]
23. Marino S, Vooijs M, van Der Gulden H, Jonkers J, Berns A. Induction of medulloblastomas in p53-null mutant mice by somatic inactivation of Rb in the external granular layer cells of the cerebellum. *Genes Dev.* 2000; 14:994–1004. [PubMed: 10783170]
24. Kobayashi H, et al. Angiocrine factors from Akt-activated endothelial cells balance self-renewal and differentiation of haematopoietic stem cells. *Nat Cell Biol.* 2010; 12:1046–1056. [PubMed: 20972423]
25. Ding L, Saunders TL, Enikolopov G, Morrison SJ. Endothelial and perivascular cells maintain haematopoietic stem cells. *Nature.* 2012; 481:457–462. [PubMed: 22281595]
26. Levesque JP, et al. Mobilization by either cyclophosphamide or granulocyte colony-stimulating factor transforms the bone marrow into a highly proteolytic environment. *Exp Hematol.* 2002; 30:440–449. [PubMed: 12031650]
27. Schober A, et al. Glial cell line-derived neurotrophic factor rescues target-deprived sympathetic spinal cord neurons but requires transforming growth factor-beta as cofactor in vivo. *J Neurosci.* 1999; 19:2008–2015. [PubMed: 10066254]
28. Saita K, et al. A catechol derivative (4-methylcatechol) accelerates the recovery from experimental acrylamide-induced neuropathy. *J Pharmacol Exp Ther.* 1996; 276:231–237. [PubMed: 8558436]
29. Callizot N, et al. Interleukin-6 protects against paclitaxel, cisplatin and vincristine-induced neuropathies without impairing chemotherapeutic activity. *Cancer Chemother Pharmacol.* 2008; 62:995–1007. [PubMed: 18270703]

30. Smeyne RJ, et al. Severe sensory and sympathetic neuropathies in mice carrying a disrupted Trk/NGF receptor gene. *Nature*. 1994; 368:246–249. [PubMed: 8145823]
31. Crowley C, et al. Mice lacking nerve growth factor display perinatal loss of sensory and sympathetic neurons yet develop basal forebrain cholinergic neurons. *Cell*. 1994; 76:1001–1011. [PubMed: 8137419]
32. Rezaee F, et al. Neurotrophins regulate bone marrow stromal cell IL-6 expression through the MAPK pathway. *PLoS One*. 2010; 5:e9690. [PubMed: 20300619]
33. Coppola V, et al. Ablation of TrkA function in the immune system causes B cell abnormalities. *Development*. 2004; 131:5185–5195. [PubMed: 15459109]
34. Kiel MJ, Yilmaz OH, Iwashita T, Terhorst C, Morrison SJ. SLAM family receptors distinguish hematopoietic stem and progenitor cells and reveal endothelial niches for stem cells. *Cell*. 2005; 121:1109–1121. [PubMed: 15989959]
35. Omatsu Y, et al. The essential functions of adipo-osteogenic progenitors as the hematopoietic stem and progenitor cell niche. *Immunity*. 2010; 33:387–399. [PubMed: 20850355]
36. Frenette PS, Pinho S, Lucas D, Scheiermann C. Mesenchymal Stem Cell: Keystone of the Hematopoietic Stem Cell Niche and a Stepping-Stone for Regenerative Medicine. *Annu Rev Immunol*. 2013
37. Yamazaki K, Allen TD. Ultrastructural morphometric study of efferent nerve terminals on murine bone marrow stromal cells, and the recognition of a novel anatomical unit: the “neuro-reticular complex”. *Am J Anat*. 1990; 187:261–276. [PubMed: 2321559]
38. Presley CA, et al. Bone marrow connexin-43 expression is critical for hematopoietic regeneration after chemotherapy. *Cell Commun Adhes*. 2005; 12:307–317. [PubMed: 16531325]
39. Armulik A, Genove G, Betsholtz C. Pericytes: developmental, physiological, and pathological perspectives, problems, and promises. *Developmental Cell*. 2011; 21:193–215. [PubMed: 21839917]
40. Franco M, Roswall P, Cortez E, Hanahan D, Pietras K. Pericytes promote endothelial cell survival through induction of autocrine VEGF-A signaling and Bcl-w expression. *Blood*. 2011; 118:2906–2917. [PubMed: 21778339]
41. Windebank AJ, Grisold W. Chemotherapy-induced neuropathy. *J Peripher Nerv Syst*. 2008; 13:27–46. [PubMed: 18346229]
42. Chruscinski AJ, et al. Targeted disruption of the beta2 adrenergic receptor gene. *J Biol Chem*. 1999; 274:16694–16700. [PubMed: 10358008]
43. Mignone JL, Kukekov V, Chiang AS, Steindler D, Enikolopov G. Neural stem and progenitor cells in nestin-GFP transgenic mice. *J Comp Neurol*. 2004; 469:311–324. [PubMed: 14730584]
44. Lucas D, Battista M, Shi PA, Isola L, Frenette PS. Mobilized hematopoietic stem cell yield depends on species-specific circadian timing. *Cell Stem Cell*. 2008; 3:364–366. [PubMed: 18940728]
45. Kamei J, Nozaki C, Saitoh A. Effect of mexiletine on vincristine-induced painful neuropathy in mice. *Eur J Pharmacol*. 2006; 536:123–127. [PubMed: 16556439]
46. Miller CL, Dykstra B, Eaves CJ. Characterization of mouse hematopoietic stem and progenitor cells. *Curr Protoc Immunol*. 2008; Chapter 22(Unit 22B):22.
47. Yuan R, Astle CM, Chen J, Harrison DE. Genetic regulation of hematopoietic stem cell exhaustion during development and growth. *Exp Hematol*. 2005; 33:243–250. [PubMed: 15676219]
48. Chow A, et al. Bone marrow CD169+ macrophages promote the retention of hematopoietic stem and progenitor cells in the mesenchymal stem cell niche. *J Exp Med*. 2011; 208:261–271. [PubMed: 21282381]

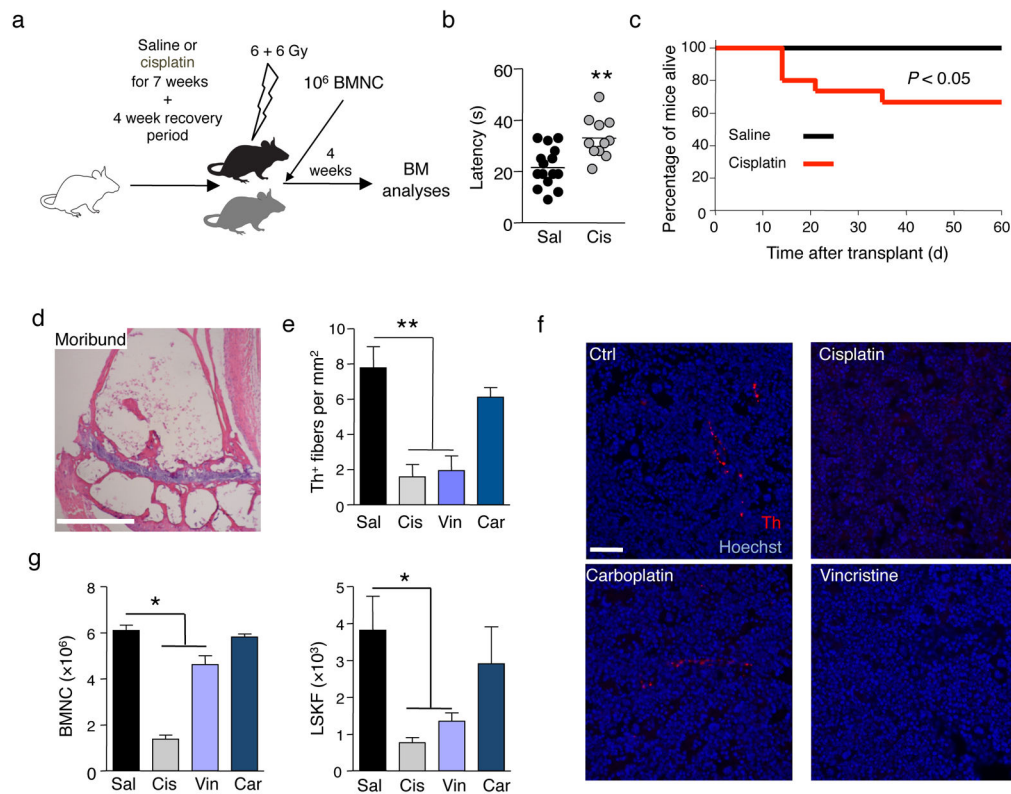


Figure 1. Neurotoxic chemotherapy induces bone marrow SNS injury and reduces engraftment after transplantation. **(a)** Experimental design to determine the effect of cisplatin on BM regeneration after transplantation. **(b)** Quantification of sensory neuropathy in mice treated with cisplatin ($n = 11$) compared to saline control ($n = 15$). **(c)** Survival of saline ($n = 15$) or cisplatin-treated ($n = 15$) mice transplanted as in a. **(d)** Representative H&E staining of femoral BM of a moribund, cisplatin-treated mouse 8 days after transplantation. Scale bar, 250 μ m. **(e)** Quantification of Th⁺ fibers in BM of mice treated with saline (Sal), cisplatin (Cis), vincristine (Vin), or carboplatin (Car), 4 weeks after the last cisplatin injection; $n = 4$. **(f)** Representative immunofluorescence images to detect the presence of Th⁺ fibers in the BM; red, Th; blue, Hoechst. Scale bar, 50 μ m. **(g)** BMNC and LSKF cells per femur in BM of mice treated with saline (Sal; $n = 13$), cisplatin (Cis; $n = 13$), vincristine (Vin; $n = 10$), or carboplatin (Car; $n = 6$), 4 weeks after transplantation of 10^6 BMNC.

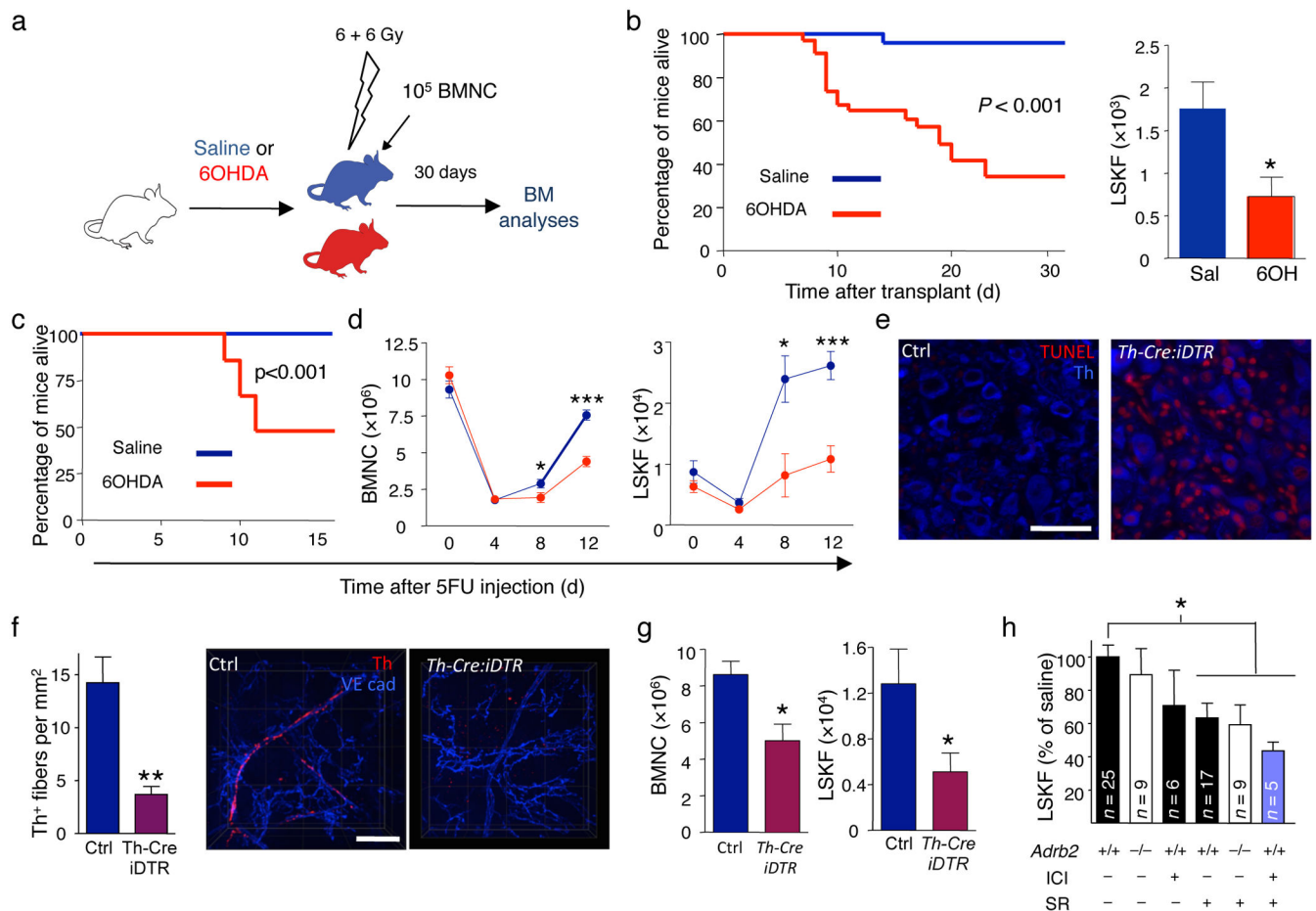


Figure 2.

The SNS regulates BM recovery. **(a)** Experimental design to determine the effect of the 6OHDA-induced SNS lesion on BM regeneration after transplantation. **(b)** The left panel shows the survival of saline ($n = 25$) or 6OHDA-treated ($n = 34$) mice transplanted using the protocol depicted in a; the right panel shows the number of LSKF cells per femur in saline ($n = 7$) or 6OHDA-treated ($n = 8$) transplanted mice 4 weeks after transplantation. **(c)**, Reduced survival of 6OHDA-sympathectomized mice ($n = 29$), compared to saline-treated controls ($n = 17$) following 5FU. **(d)** The left panel shows the number of BMNC per femur in mice treated with saline (blue) or 6OHDA (red) at days 0 ($n = 5-8$), 4 ($n = 15-16$), 8 ($n = 13-15$) and 12 ($n = 21-22$) after 5FU injection; the right panel shows the number of LSKF cells per femur in mice treated with saline (blue) or 6OHDA (red) at days 0 ($n = 5-7$), 4 ($n = 5$), 8 ($n = 4-5$) and 12 ($n = 6-11$) after 5FU injection. **(e)** Representative immunofluorescence images showing induction of apoptosis (TUNEL, red) in Th⁺ sympathetic neurons (blue) in superior cervical ganglia from WT or *Th-Cre:iDTR* mice 12h after diphtheria toxin injection. Scale bar 50 μ m. **(f)** Quantification of BM Th⁺ fibers in WT or *Th-Cre:iDTR* mice 12 days after 5FU injection ($n = 4$); right panels show representative whole-mount immunofluorescence staining in the sternum; Th (red); VE cadherin (vessels, blue). Scale bar, 50 μ m. **(g)** BMNC and LSKF cells per femur in the BM of *Th-Cre:iDTR* or *iDTR* and *Th-Cre* (Ctrl) mice 12 days after DT treatment and 5FU injection ($n = 6$). **(h)**

Number of LSKF cells per femur in the BM of WT or *Adrb2*^{-/-} mice treated with saline, SR59230A (SR; β 3-AR blocker) or ICI118551 (ICI; β 2-AR blocker).

Author Manuscript

Author Manuscript

Author Manuscript

Author Manuscript

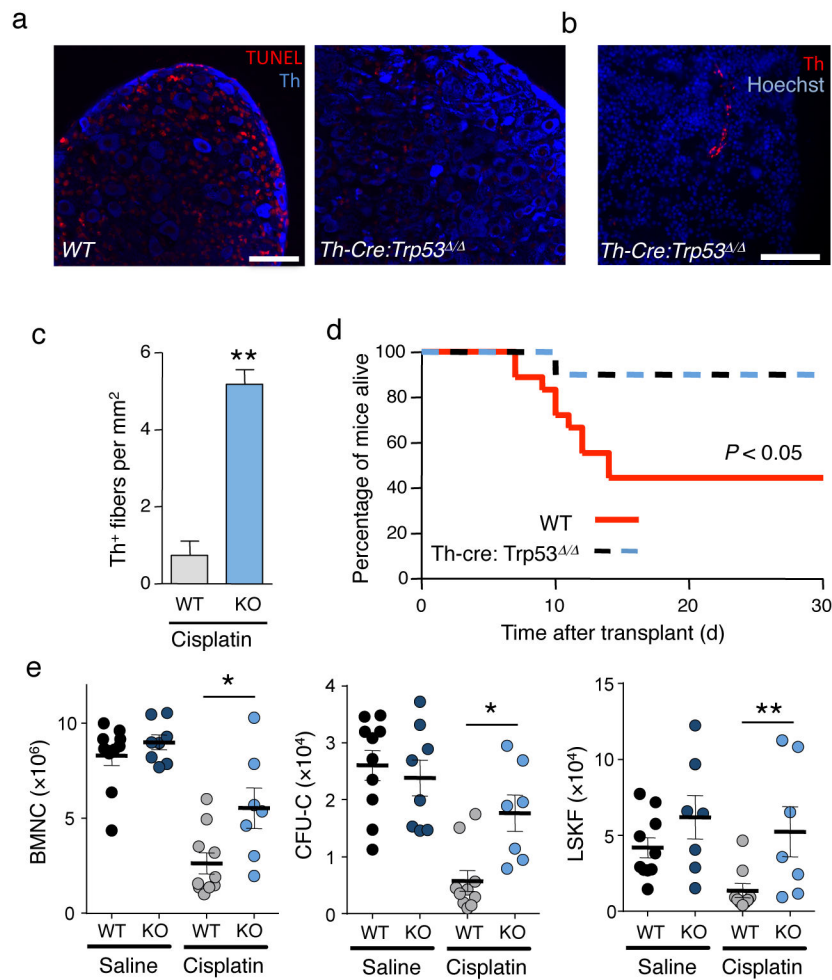
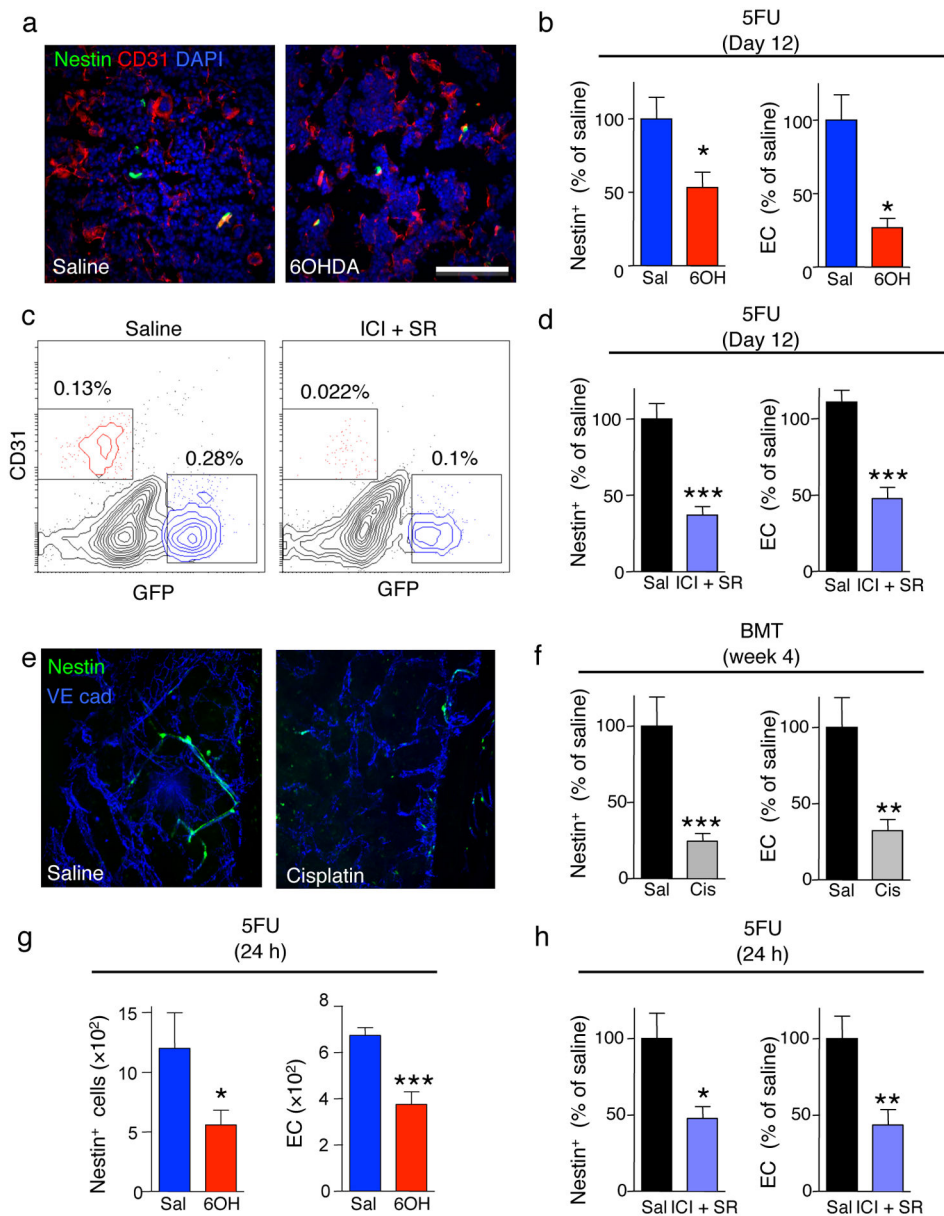


Figure 3. Reduced BM recovery after cisplatin chemotherapy is due to SNS injury. **(a)** Representative immunofluorescence images of superior cervical ganglia showing apoptosis by TUNEL stain (red) in sympathetic neurons (Th, blue) of wild-type or *Th-Cre:Trp53^{Δ/Δ}* mice 12h after cisplatin injection. Scale bar 25 μ m **(b)** Representative immunofluorescence image of Th⁺ fibers in the BM of a *Th-Cre:Trp53^{Δ/Δ}* mouse after cisplatin. Scale bar, 50 μ m. **(c)** Quantification of Th⁺ fibers in the BM of cisplatin-treated control (WT) or *Th-Cre:Trp53^{Δ/Δ}* (KO) mice, 4 weeks after the last cisplatin injection. ($n = 3$) **(d)** Overall survival of wild-type (WT; $n = 18$) or *Th-Cre:Trp53^{Δ/Δ}* ($n = 10$) mice after cisplatin treatment and transplantation ($n = 6-12$). **(e)** BMNC, CFU-C and LSKF cells per femur in the BM of WT or *Th-Cre:Trp53^{Δ/Δ}* (KO) littermates treated with saline or cisplatin 4 weeks after transplantation ($n = 4-10$).

**Figure 4.**

β -adrenergic signals protect the niche from genotoxic insult. **(a)** Representative immunofluorescence BM images of saline- or 6OHDA-treated *Nestin-gfp* mice, 12 days after 5FU injection. Green: Nestin-GFP⁺ cells; red, CD31 (endothelial cells); blue, DAPI. **(b)** Number of Nestin-GFP⁺ and endothelial cells (EC) per femur in saline or 6OHDA-treated *Nestin-gfp* mice 24h or 12 days after 5FU injection ($n = 6-8$). **(c)** Representative flow cytometry plots (gated on live CD45⁻Ter119⁻ cells) showing nestin-GFP⁺ and CD31⁺ endothelial cells in mice treated with saline or ICI112851 (ICI; β 2-AR blocker) and SR59230A (SR; β 3-AR blocker), 12 days after 5FU injection. $n = 5$ **(d)** Number of nestin-GFP⁺ and endothelial cells (EC) per femur in mice treated as in c. **(e)** whole-mount immunofluorescence staining of the sternum; green: nestin-GFP⁺ cells; blue: VE cadherin (vessels); of mice treated with saline (sal) or cisplatin (cis) 4 weeks after transplantation of

10^6 BMNC. **(f)** Number of Nestin-GFP⁺ and endothelial cells (EC) per femur in mice treated as in e. **(g, h)** Number of Nestin-GFP⁺ and EC per femur in mice treated with saline or 6OHDA ($n = 6-7$) **(g)** or ICI112851 and SR59230A **(h)** 24 h after 5FU injection ($n = 8$).

Author Manuscript

Author Manuscript

Author Manuscript

Author Manuscript

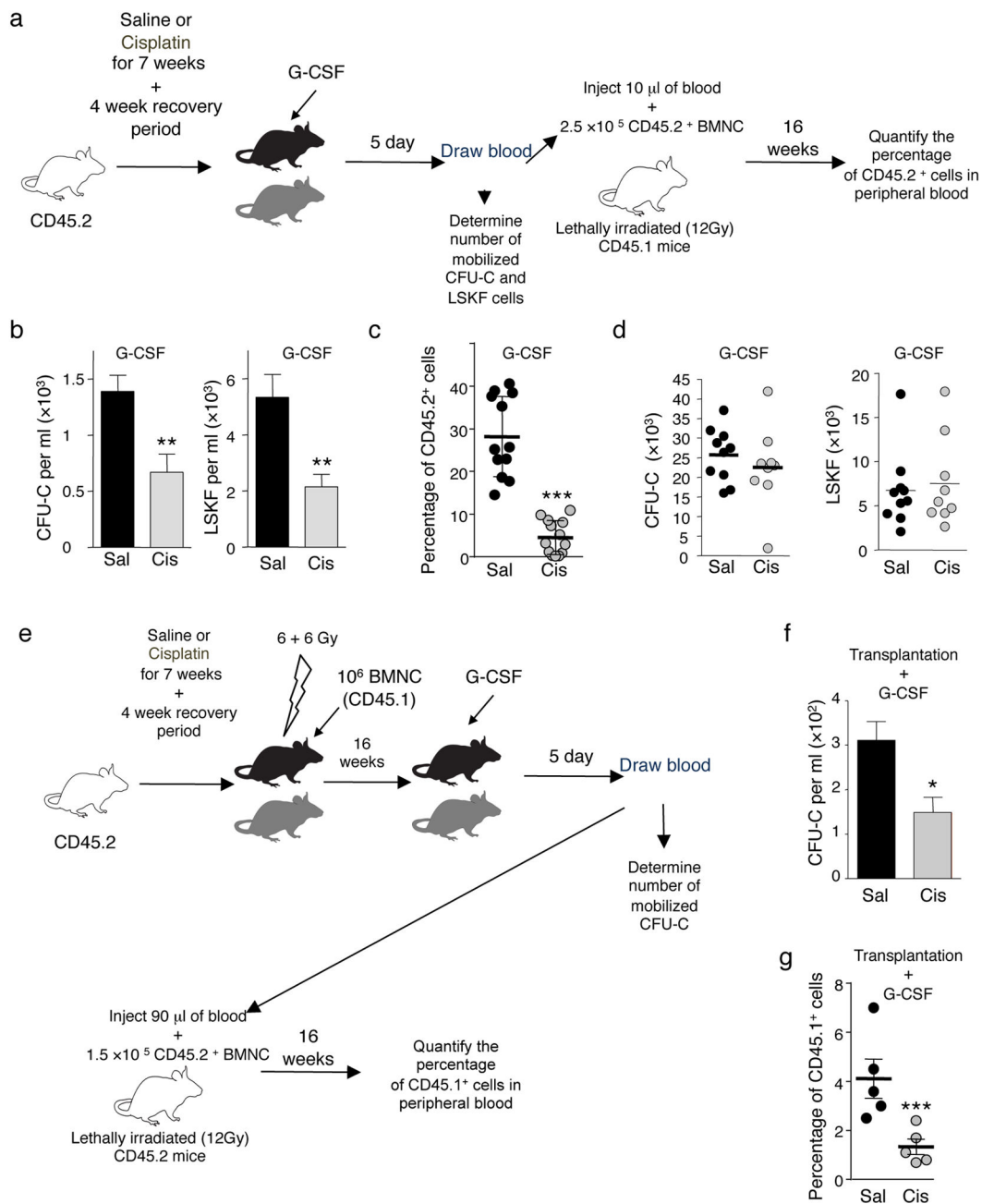


Figure 5.

Bone marrow SNS injury impairs progenitor mobilization. **(a)** Experimental design to determine whether cisplatin treatment prevents HSC mobilization. **(b)** CFU-C (right panel) and LSKF (left panel) counts in blood after G-CSF-induced mobilization in cisplatin or saline-treated mice ($n = 10$). **(c)** Competitive repopulation assay showing the percentage of CD45.2+ cells in the blood of CD45.1+ mice transplanted as indicated in a. **(d)** Number of total CFU-C (left panel) or LSKF (right panel) per femur in saline or cisplatin-treated mice, mobilized with G-CSF as indicated in a ($n = 9-10$). **(e)** Experimental design to assess whether the HSC mobilization defect in cisplatin-treated mice originates from the

microenvironment. **(f)** CFU-C counts in blood after G-CSF-induced mobilization in cisplatin- or saline-treated mice transplanted and mobilized as indicated in e ($n = 7-9$). **(g)** Competitive repopulation assay showing the percentage of CD45.1⁺ cells in the blood of CD45.2⁺ mice transplanted as indicated in e.

Author Manuscript

Author Manuscript

Author Manuscript

Author Manuscript

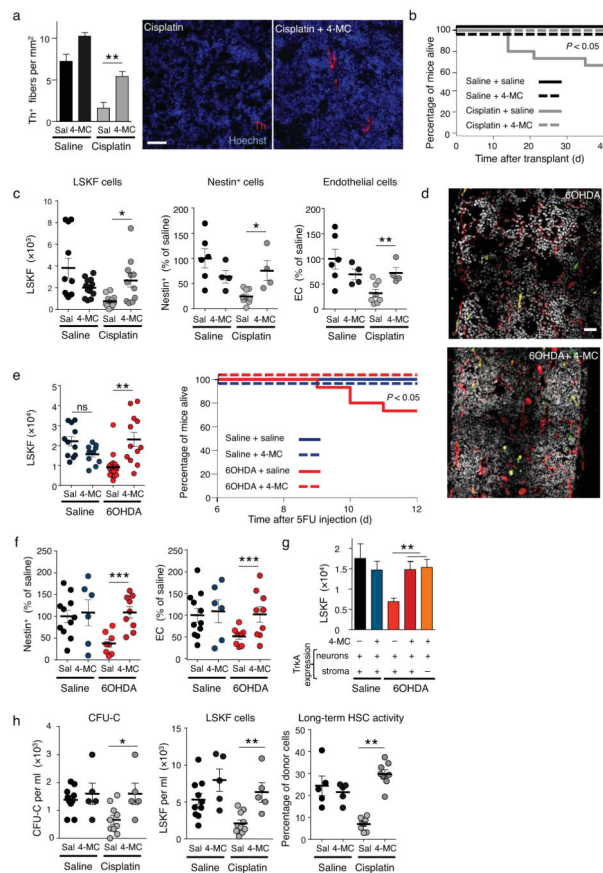


Figure 6.

Neuroprotection restores normal BM engraftment and mobilization. **(a)** Quantification of Th⁺ fibers in the BM of saline or cisplatin-treated mice after 4-MC neuroprotection, 4 weeks after the last cisplatin injection ($n = 4-6$). Representative immunofluorescence images showing Th⁺ fibers in the BM; red, Th; blue, DAPI. Scale bar, 40 μ m. **(b)** Overall survival of saline or cisplatin-treated mice after 4-MC neuroprotection and transplantation ($n = 8-15$). **(c)** The left panel shows the number of LSKF cells per femur in the BM of the mice analyzed in **(a)** ($n = 11-13$). Statistical comparisons were performed using the Mann Whitney method. The center and right panels show the percentage of Nestin-GFP⁺ or endothelial cells per femur in *Nestin-Gfp* mice treated with saline, cisplatin and 4-MC, 4 weeks after BM transplantation ($n = 4$). **(d)** Representative composite patchwork of femoral sections, 12 days after 5FU injection, of *Nestin-gfp* mice treated with saline, 6OHDA and 4-MC; red: CD31, white: DAPI, green: nestin-GFP⁺ cells. Scale bar, 100 μ m **(e)** Number of LSKF cells per femur in mice treated with saline, 6OHDA and 4-MC, 12 days after 5FU injection ($n = 5-7$). Statistical comparisons were performed using the Mann Whitney method; the right panel shows the overall survival of saline or 6OHDA-treated mice after 4-MC neuroprotection and 5FU injection ($n = 8-29$). **(f)** Percentage of nestin-GFP⁺ or endothelial cells per femur in *Nestin-Gfp* mice treated with saline, 6OHDA and 4-MC, 12 days after 5FU injection ($n = 5-11$). **(g)** Number of LSKF cells per femur in WT or *Tal-Cre:TrkA^{Neo/Neo}* mice treated with 6OHDA and 4-MC, 12 days after 5FU injection ($n = 3-8$). **(h)** CFU-C and LSKF counts per ml of blood in saline (Sal) or cisplatin-treated mice

after 4-MC neuroprotection and G-CSF mobilization; the right panel indicates the percentage of CD45.2⁺ cells in peripheral blood of CD45.1⁺ mice transplanted with 10 μ l of G-CSF mobilized blood and 2.5×10^5 competitor CD45.1⁺ BMNC.

Author Manuscript

Author Manuscript

Author Manuscript

Author Manuscript